ELSEVIER

Applied Surface Science 109/110 (1997) 189–193

applied surface science

Laser micromachining of free-standing structures in SiO_2-covered silicon

M. Allard, S. Boughaba, M. Meunier *

Groupe des Couches Minces (GCM) and Département de Génie Physique, École Polytechnique de Montréal, C.P. 6079, Succursale 'Centre-Ville', Montréal, Que., Canada H3C 3A7

Received 5 June 1996; accepted 26 August 1996

Abstract

Tunnels and free-standing microstructures were fabricated in SiO_2-covered silicon, using a laser-based micromachining technique. We employed a focused CW Ar^+ laser beam, at a wavelength of 514 nm, to melt the silicon and provoke its etching in a chlorine ambient; the oxide layer is transparent to the laser beam, and is not affected by the process. Tunnels were etched for different incident beam powers and scanning speeds, at a chlorine pressure of 500 Torr. For an incident power of 1.6 W and a scanning speed of 25 $\mu m/s$, tunnels 7.5 μm deep and 3.6 μm wide were obtained. For a given scanning speed, defects were observed at the tops of the tunnels after a critical length, around 400 μm for a scanning speed of 5 $\mu m/s$, ripples and tiny holes were generated in the oxide film. The defect-free length of the tunnels, L_c, was investigated as a function of the reciprocal of the scanning speed, $(V_{scan})^{-1}$; for an incident laser power of 1.2 W, $(L_c V_{scan}) = 2400$ $\mu m^2/s$. Furthermore, various free-standing microstructures, cantilevers and square membranes, were successfully machined.

1. Introduction

The micromachining of silicon is an essential processing step in the fabrication of micro-electro-mechanical systems (MEMS) [1,2]. It is conventionally carried out using photolithography, followed by anisotropic wet etching or reactive ion etching (RIE) [3,4]. Such a conventional approach has serious limitations [5]. A possible alternative to these techniques is laser micromachining, which refers to the laser-induced etching of silicon in a chlorine ambient [5–8]. A laser beam is tightly focused onto a silicon substrate to locally heat the surface up to the melting temperature. The localized melted silicon defines a reaction zone where the dissociation of the chlorine molecules occurs, leading to the formation of silicon-containing volatile species, resulting in localized etching. By moving the substrate horizontally in the focal plane, direct-etching of patterns can be generated.

If a thin silicon dioxide (SiO_2) layer is grown on the silicon substrate, free-standing structures can be machined by simply etching and patterning the silicon underneath the oxide film [5,6,8]. Indeed, SiO_2 is transparent to wavelengths in the range of 488–514 nm (CW Ar^+), the SiO_2/Si etch rate ratio in chlorine is very small, and the melting temperature of silicon is lower than that of SiO_2. Using this process, tunnels and cavities, which may find application as

* Corresponding author. E-mail: meunier@phys.polymtl.ca.

0169-4332/97/$17.00 Copyright © 1997 Elsevier Science B.V. All rights reserved.
PII S0169-4332(96)00658-7

microfluidic devices parts, could be fabricated. Furthermore, free-standing structures such as cantilevers, beams or membranes may also be machined and used as parts of MEMS.

2. Experimental

The experimental set-up and working procedure have already been described in detail elsewhere [5,8]. Briefly, the TEM_{00} beam of a CW Ar^+ laser, operating at a wavelength of 514 nm, is focused by a microscope objective into a reaction cell containing the substrate. The measured beam spot diameter $(1/e^2)$ at the substrate surface is 7 μm. Moving the cell, and therefore the substrate, is assured by a computer-controlled x–y stage.

The substrates used were p-doped (1–10 Ωcm) $\langle 100 \rangle$ silicon wafers, on which a 0.38 μm-thick oxide layer was thermally grown (1280°C) in a dry O_2–N_2 atmosphere. Prior to use, the samples were cleaned by successive immersing in hot trichloroethane–acetone–isopropanol.

Once a sample was placed in the cell, a primary vacuum (10^{-3} Torr) was established in the chamber. Prior to the introduction of the chlorine, an opening of 1500×50 μm^2 was made in the SiO_2 film by laser ablation. The role of this opening is to assure the arrival and renewal of the reactive gas at the reaction zone. The SiO_2 film ablation was accomplished by first bringing the SiO_2/Si interface to the focal plane of the objective; then the laser was turned on at an incident power of 1.35 W and its beam scanned in adjacent paths, 1 μm apart (raster scan). The cell was then filled with Cl_2 to a pressure of 500 Torr. To etch a tunnel, the laser beam was moved from the ablated area into the SiO_2-covered silicon. Laser powers up to 1.75 W were used for the etching step. In order to make free-standing microstructures, areas surrounding the parts to be left intact were first ablated; then the underlying silicon was etched by successive scans, 0.5 μm apart.

The widths and depths of the tunnels were measured by observing the cross-sections (at 1 mm from the opening) using a scanning electron microscope (SEM). SEM was also used, in conjunction with optical and atomic force microscopies, to analyze the defects generated on the top of the oxide layer.

3. Laser micromachining of tunnels

Fig. 1 shows a SEM picture of the cross-section of two tunnels, etched using incident laser powers of 1.39 W (left) and 1.33 W (right), at a scanning speed of 25 μm/s. The tunnels have a depth of 4.5 μm (left, 1.39 W) and 4.3 μm (right, 1.33 W), and a width at the top of 3.2 and 2.9 μm, respectively. For these experimental conditions, no effect of the etching process is observed on the oxide layer.

Similar tunnels were etched for incident laser powers ranging from 0.9 to 1.75 W. Below 0.9 W, no etching was observed. For higher powers, the depth of the tunnels increased rapidly as it is shown in Fig. 2; depths up to 9 μm were obtained at an incident power of 1.7 W and a scanning speed of 25 μm/s. No significant increase in the top width of the tunnels was measured. The error bars introduced in Fig. 2 were obtained by measuring the depth of 25 tunnels, etched at an incident power of 1.2 W and scanning speed of 25 μm/s. The mean depth was 3.9 μm and the bar amplitude corresponds to twice the standard deviation, found to be 0.7 μm, assuming it to be independent of the incident power.

The top observation of the etched tunnels, through the SiO_2 layer, using the optical microscope, combined with the SEM cross-section investigation, permitted the observation of a cyclic phenomenon, characteristic of the etching process. For a given set of experimental conditions, the etched tunnels, which

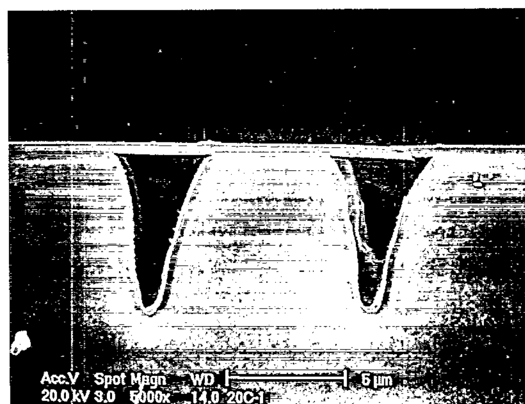

Fig. 1. SEM picture of two tunnels etched at an incident laser power of 1.39 W (left) and 1.33 W (right), a Cl_2 pressure of 500 Torr, and a scanning speed of 25 μm/s.

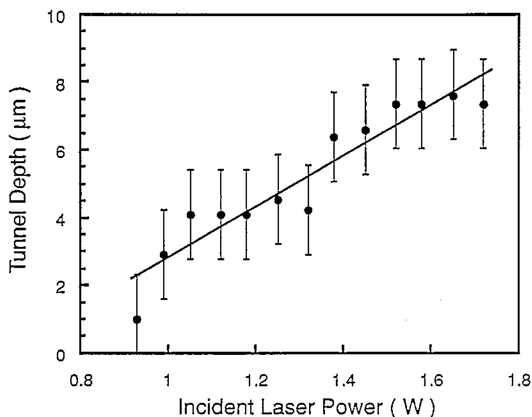

Fig. 2. Dependence of the etched tunnel depth on the incident laser power. Cl_2 pressure: 500 Torr; scanning speed: 25 μm/s.

started from the ablated area, first showed regular widths and sections up to a critical length, L_c. Beyond this length, the tunnels narrowed and became shallower for a short distance, before they recovered their initial regular widths and cross-sections. This bottleneck phenomenon was reproducible along the etched tunnels. It is schematically described in the insert of Fig. 3.

On closer examination using the SEM, ripples and tiny holes ($\sim$ 100 nm diameter) were observed in the oxide layer, over the region where the tunnels narrow. An AFM investigation confirmed the presence of such defects. These defects could be related to the formation of volatile species, such as SiO, at the SiO_2/Si interface [9]. In our configuration, these species may, on one hand, exercise a pressure on the SiO_2 top layer, inducing localized stress, which could be related to the ripples observed. On the other hand, their diffusion toward the top surface may result in the formation of so-called chimneys [9], which could be associated to the holes. It must be emphasized that these defects were observed only at the bottleneck regions of the tunnels. To account for this, one has to consider that the etching process involves two competing, parallel, reactional paths at the etching front: (i) The silicon reaction with the chlorine radicals to form volatile $SiCl_4$, and (ii) the formation of volatile SiO species at the SiO_2/Si interface. As long as the arrival and renewal of the Cl_2 gas at the etching front is assured, path (i) may be the prevailing one. When the Cl_2 diffusion-limited regime is reached, after a certain length of the tunnel, the amount of available reactant gas molecules is not sufficient to rapidly react with the molten silicon through $SiCl_4$ species, and the SiO formation path prevails, resulting in chimneys. These channels are, in turn, new ways for the chlorine to reach the melted region and, therefore, to initiate the etching of a new regular segment of the tunnel. It must be emphasized that path (ii) may account for the ablation of the SiO_2 film under vacuum.

To determine, for practical applications, the longest tunnels with regular depths and widths, we measured the length of the initial regular segments of tunnels etched at different scanning speeds. This critical length was found to be strongly dependent on the reciprocal of the scanning speed, as it is shown in Fig. 3. The insert is a schematic of the bottleneck cyclic phenomenon. The critical length L_c is proportional to the reciprocal of the scanning speed, $(V_{scan})^{-1}$, such that the slope $(L_c V_{scan}) = 2400$ $\mu m^2/s$. At very slow scanning speeds (5 μm/s), lengths of over 400 μm are obtained. This dependence could primarily be related to the dependence of the etched depth, i.e., tunnel vertical section, on the scanning speed.

To account for the proportional relationship between the critical length, L_c (μm), and the inverse

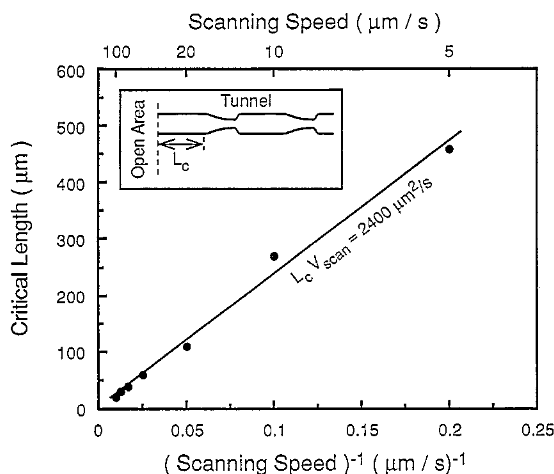

Fig. 3. Dependence of the critical length, L_c, of the etched tunnels on the scanning speed, V_{scan}. Cl_2 pressure: 500 Torr; incident laser power: 1.2 W. The insert is a schematic of the bottleneck cyclic phenomenon.

of the scanning speed, $(V_{scan})^{-1}$ $(\mu m/s)^{-1}$, one can establish an analogy with conventional chemical vapor deposition (CVD), in which diffusive transport of reactant molecules occurs through a boundary layer, δ (μm) [10]. In the case of a diffusion-limited regime, the etching rate R ($\mu m^3/s$) is approximately given by

$$R = (SD/\rho_{Si})(N_{Cl_2}/\delta) = SV_{scan}$$

where D (cm^2/s) is the Cl_2 diffusion coefficient assumed to be constant, S (μm^2) is the vertical cross-section of the tunnel, ρ_{Si} is the Si density (5×10^{22} cm^{-3}) and N_{Cl_2} is the Cl_2 molecular density outside the boundary layer ($\approx 1.6 \times 10^{19}$ cm^{-3} at 500 Torr and 300 K). In our case, we assume that the length of an etched tunnel could be associated to the boundary layer δ, through which Cl_2 has to diffuse. As long as the chlorine supply to the reaction zone is not limiting, i.e., for small values of δ, the etching is determined by surface reactions. When the tunnel reaches a critical length $\delta = L_c$ so that the diffusion of the Cl_2 through the reaction products is appreciably reduced, the process becomes diffusion-limited. In this case, the product

$$V_{scan} L_c = N_{Cl_2} D/\rho_{Si}$$

is constant for a given set of processing conditions, as was experimentally observed (Fig. 3). Moreover, using our experimental values, we find that $D \cong 0.08$ cm^2/s, in good agreement with an estimate of the Cl_2 self diffusion coefficient (0.12 cm^2/s) [11].

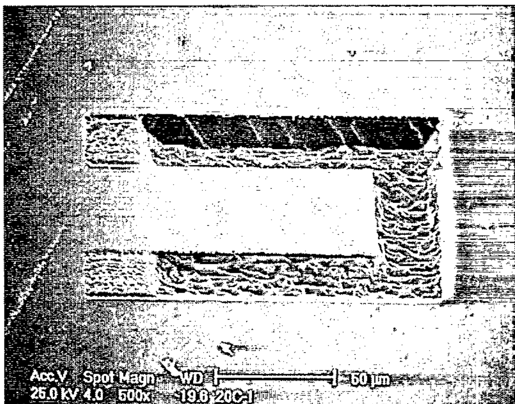

Fig. 4. A 40×100 μm^2 cantilever machined at an incident laser power of 1.33 W and a scanning speed of 50 $\mu m/s$.

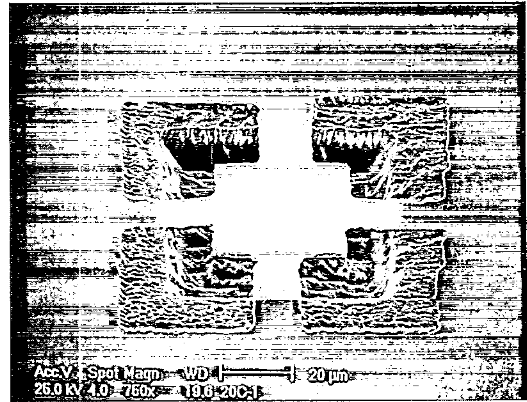

Fig. 5. A 36×36 μm^2 free-standing membrane machined at an incident laser power of 1.33 W and a scanning speed of 50 $\mu m/s$.

4. Laser micromachining of free-standing structures

Using the technique described above, free-standing microstructures can be made in the oxide layer. An example of such a structure is shown in Fig. 4, where a 40×100 μm^2 cantilever was etched using an incident power of 1.33 W, at a scanning speed of 50 $\mu m/s$. The total fabrication time was about 15 min. On the lateral sides of the anchorage region, the oxide was ablated, but no etching was performed. To insure that the cantilever was completely free from the underlying silicon depression, the oxide was etched in a $HF:H_2O$ (1:10) solution for 10 min. No silicon remained under the cantilever; the bottom silicon surface was, within its roughness variation, uniformly at the same level. The measured depth of the depression was 15 μm. It must be emphasized that, because of the raster scan, chlorine does not have to diffuse along any tunnel path to get to the etching front. As a consequence, no defects are induced in the oxide layer when performing such structures.

Fig. 5 shows another microstructure. This is a 36×36 μm^2 membrane in the oxide layer, anchored on all four sides to the surrounding substrate. The etching was performed at a laser power of 1.33

W and a scanning speed of 50 μm/s. The fabrication time was less than 10 min.

5. Conclusion

Argon-ion laser micromachining was used to make tunnels and free-standing microstructures in SiO_2-covered silicon substrates. Tunnels having a width around 3.5 μm and depths up to 9 μm were etched. The critical length over which defect-free tunnels could be machined was found to be inversely proportional to the scanning speed. A critical length of 400 μm was measured for a scanning speed of 5 μm/s.

A cantilever and a square membrane were presented as examples of possible free-standing microstructures which can be constructed by this technique.

Acknowledgements

The authors thank Jean-Paul Lévesque for his technical assistance, Mario Caron for the SEM analysis, and Suzie Poulin for carrying out the AFM investigations. We are also indebted to Bing Shen for his involvement in the preliminary work on the process development. We also want to acknowledge the financial support of the Natural Sciences and Engineering Research Council of Canada (NSERC) and Fonds pour la Formation des Chercheurs et l'Aide à la Recherche (FCAR) du Québec.

References

[1] M. Mehregany, IEEE Circuits Devices Mag. 9 (1993) 14.
[2] M. Mehregany, in: Integrated Optics and Microstructures, Eds. M. Tabib-Azar and D.L. Polla, Proc. SPIE 1793 (1993) 2.
[3] K.E. Petersen, Proc. IEEE 70(5) (1982) 420.
[4] C. Linder, L. Paratte, M.-A. Gretillat, V.P. Jaecklin and N.F. de Rooij, J. Micromech. Microeng. 2 (1992) 122.
[5] B. Shen, M. Allard, S. Boughaba, R. Izquierdo and M. Meunier, Can. J. Phys., to be published.
[6] T.M. Bloomstein and D.J. Ehrlich, in: Technical Digest of Transducers '91 (IEEE, New York, 1991) p. 507.
[7] T.M. Bloomstein and D.J. Ehrlich, J. Vac. Sci. Technol. B 10 (1992) 2671.
[8] B. Shen, R. Izquierdo and M. Meunier, in: Laser-Assisted Fabrication of Thin Films and Microstructures, Ed. I.W. Boyd, Proc. SPIE 2045 (1994) 91.
[9] G. Auvert, in: Beam–Solid Interactions: Fundamentals and Applications, Mater. Res. Soc. Symp. Proc., Vol. 279, Eds. M. Nastasi, L.R. Harriot, N. Herbots and R.S. Averback (Materials Research Society, Pittsburgh, 1993) p. 711.
[10] J. Bloem and L.J. Giling, in: Current Topics in Materials Science, Ed. E. Kaldis, Vol. 1 (North-Holland, Amsterdam, 1978) p. 147.
[11] R.H. Perry and D.W. Green, Perry's Chemical Engineers Handbook, 6th ed. (McGraw-Hill, New York, NY, 1984) pp. 3–285.